Maturation enhances fluid shear-induced activation of eNOS in perfused ovine carotid arteries

Charles Ray White, Mohammad Wael Hamade, Koushan Siami, Melody M. Chang, Anandit Mangalwadi, John A. Frangos and William J. Pearce

AJP - Heart 289:2220-2227, 2005. First published May 27, 2005; doi:10.1152/ajpheart.01013.2004

AJP - Heart and Circulatory Physiology publishes original investigations on the physiology of the heart, blood vessels, and lymphatics, including experimental and theoretical studies of cardiovascular function at all levels of organization ranging from the intact animal to the cellular, subcellular, and molecular levels. It is published 12 times a year (monthly) by the American Physiological Society, 9650 Rockville Pike, Bethesda MD 20814-3991. ISSN: 0363-6135, ESSN: 1522-1539. Visit our website at http://www.the-aps.org/.

Am J Physiol Heart Circ Physiol 289: H2220–H2227, 2005.
First published May 27, 2005; doi:10.1152/ajpheart.01013.2004.

Maturation enhances fluid shear-induced activation of eNOS in perfused ovine carotid arteries

Charles Ray White,[1,2] Mohammad Wael Hamade,[1] Koushan Siami,[1] Melody M. Chang,[1] Anandit Mangalwadi,[1] John A. Frangos,[2] and William J. Pearce[1]

[1]*Center for Perinatal Biology, Loma Linda University, Loma Linda; and* [2]*La Jolla Bioengineering Institute, La Jolla, California*

Submitted 4 October 2004; accepted in final form 26 May 2005

White, Charles Ray, Mohammad Wael Hamade, Koushan Siami, Melody M. Chang, Anandit Mangalwadi, John A. Frangos, and William J. Pearce. Maturation enhances fluid shear-induced activation of eNOS in perfused ovine carotid arteries. *Am J Physiol Heart Circ Physiol* 289: H2220–H2227, 2005. First published May 27, 2005; doi:10.1152/ajpheart.01013.2004.—The present study tests the hypothesis that age-dependent increases in endothelial vasodilator capacity are due to maturational increases in endothelial nitric oxide (NO) synthesis and release. Intact 4-cm carotid artery segments taken from term fetal lambs and nonpregnant adult sheep were perfused by using a closed system that enabled independent control of flow and inflow pressure and facilitated complete recovery of all NO released. Fluid shear stress induced a graded release of NO (in nmol $NO \cdot min \cdot cm^{-2}$ of luminal surface area) that was significantly greater in adult (890 ± 140) than in fetal (300 ± 40) carotid arteries at corresponding values of shear stress (5.9 ± 0.3 dyn/cm^2) but was independent of inflow pressure in both age groups. These age-related differences in NO release were not attributable to corresponding differences in endothelial NO synthase (eNOS) abundance, as eNOS protein levels (in ng of eNOS/cm^2 of luminal surface area) were similar in adult (14 ± 2) and fetal (12 ± 1) arteries. Adult (80 ± 15) and fetal (89 ± 32) levels of eNOS mRNA (in 10^6 copies/cm^2 of luminal surface area) were also similar. However, when NO release was normalized relative to the associated mass of eNOS protein to estimate eNOS-specific activity in situ, this value (in nmol $NO \cdot \mu g$ of $eNOS^{-1} \cdot min^{-1}$) was significantly greater in adult (177 ± 44) than in fetal (97 ± 36) arteries when the endothelium was maximally activated by A-23187. Similarly, the slope of the relation between fluid shear stress and estimated eNOS-specific activity (in nmol $NO \cdot \mu g$ of $eNOS^{-1} \cdot min^{-1}$ per dyn/cm^2) was also significantly greater in adult (6.8 ± 0.1) than in fetal (2.9 ± 0.1) arteries, which suggests that eNOS may be more sensitive to or more efficiently coupled to activating stimuli in adult compared with fetal arteries. We conclude that maturational increases in endothelial vasodilator capacity are attributable to age-dependent increases in NO release secondary to elevated eNOS-specific activity and involve more efficient coupling between endothelial activation and enhancement of eNOS activity in adult compared with fetal arteries.

endothelium; endothelial nitric oxide synthase; postnatal; vasodilation; cardiovascular regulation

ONE OF THE MOST SIGNIFICANT advances in neonatal medicine during the past two decades is the ability to maintain extremely small infants using modern neonatal intensive care unit technology (19). Experience with these small patients has helped advance the view that basic patterns of cardiovascular regulation are quite different in neonates and adults (5, 28). Whereas considerable investigative effort has focused on mechanisms that regulate cardiac and vascular contractility in neonates (3), far less attention has focused on mechanisms of vasodilatation in the fetus and neonate, and in particular, those mediated by the vascular endothelium. Indeed, among the many thousands of publications that have focused on endothelial function, <1% have examined endothelium-dependent vasodilatation in immature arteries of any kind.

A key challenge for studies of endothelium-dependent vasodilatation is the general characteristic that endothelial function is highly heterogeneous among different vascular beds (31). In addition, endothelial phenotype is highly dynamic and sensitive to physiological modulation by hormones and shear stress and to pathophysiological modulation by inflammation and injury (27). Without doubt, endothelial culture systems have been highly valuable in establishing the basic mechanisms governing endothelial function (23), but the tendency for endothelial cells to change phenotype under culture conditions (15) dictates that elucidation of the effects of postnatal maturation on endothelial vasodilator function is best realized by using intact arteries.

Among the relatively few studies that have examined endothelial vasodilator function in immature arteries, a finding common across species is that the magnitude of vasodilatation increases with postnatal age (9, 18, 21, 30). This effect suggests that postnatal maturation increases either the endothelial release of vasodilator molecules and/or vascular sensitivity to the vasodilators released. In contrast to some other preparations (37), nitric oxide (NO) is the primary vasodilator molecule released from the endothelium of both mature and immature ovine carotid arteries (33); therefore, the combined evidence suggests that in these arteries, postnatal maturation must increase either vascular sensitivity to NO and/or endothelial NO release (34). As we have demonstrated previously (22), vasorelaxant sensitivity to NO is not increased by postnatal maturation, which suggests that maturation enhances NO release in response to endothelial activation. The present studies were designed to explore this hypothesis.

If, indeed, postnatal maturation enhances endothelial NO release, there are at least three possible mechanisms that could mediate this effect. First, maturation could simply increase endothelial NO synthase (eNOS) abundance. Second, maturation could increase the specific activity of eNOS. Third, maturation could enhance the ability of physiological and pharma-

Address for reprint requests and other correspondence: W. J. Pearce, Center for Perinatal Biology, Loma Linda Univ., Loma Linda, CA 92350 (e-mail: wpearce@llu.edu).

The costs of publication of this article were defrayed in part by the payment of page charges. The article must therefore be hereby marked "*advertisement*" in accordance with 18 U.S.C. Section 1734 solely to indicate this fact.

cological perturbations to activate eNOS. To test these three corollaries of our main hypothesis, we measured NO release from isolated perfused ovine carotid arteries from term fetal lambs and nonpregnant adult sheep. Western blots for eNOS were used to assess the effects of postnatal maturation on both eNOS abundance and specific activity. To examine the coupling between endothelial activators and NO production, endothelial NO release was stimulated physiologically by exposing the arteries to varying levels of fluid shear stress and inflow pressure. NO release was also stimulated physiologically by the receptor-dependent endothelium activator ADP and pharmacologically by the receptor-independent activator A-23187, which is a calcium ionophore. Given that endothelial NO release has not been previously studied in intact fetal arteries of any type, the present studies offer a novel perspective of how postnatal maturation modulates endothelial NO release.

METHODS

General preparation. All procedures and protocols used in the present studies were approved by the Animal Research Committee of Loma Linda University and followed the guidelines put forth in the National Institutes of Health's *Guide for the Care and Use of Laboratory Animals*. Common carotid arteries were obtained from young, nonpregnant female sheep (18–24 mo old) and fetal lambs (139–141 days gestation) of either sex. Animals were anesthetized with thiamylal (10 mg/kg), and the common carotid arteries were isolated and removed without stretching and were then bubbled with 95% O_2-5% CO_2 in a modified Krebs-bicarbonate solution that contained (in mM) 112 NaCl, 25.6 $NaHCO_3$, 5.56 dextrose, 5.17 KCl, 2.49 $MgSO_4$, 1.60 $CaCl_2$, and 0.027 disodium EDTA at pH 7.4. The arteries were carefully cleaned of surrounding adipose and connective tissue and cut into multiple individual segments 4 cm in length. To determine the diameters of the interior lumens of artery segments designated for perfusion, coronal sections were placed under buffer on slides and digitally imaged with a charge-couple device camera. Artery circumference, wall thickness, and diameter were determined via image analysis with Image-Pro Plus software. Luminal surface area was calculated as the product of artery circumference and segment length for each segment studied. For all perfused artery segments, corresponding adjacent artery segments were flash frozen in liquid nitrogen and stored at −70°C for subsequent Western blot determination of eNOS content (see *Quantitative Western blot analysis of eNOS*). Artery segments designated for immunohistochemistry were processed immediately (see *Immunohistochemistry for eNOS*).

Artery perfusion. One end of each artery segment was mounted on a 12-gauge cannula and inserted into a sealed 3-ml chamber (Fig. 1). The segments were perfused by peristaltic pump (at 60–80 pulses/min) with Na-HEPES buffer (that contained 10 mM Na-HEPES, 122 mM NaCl, 5.2 mM KCl, 2.5 mM $MgSO_4$, 21 mM dextrose, 1.6 mM $CaCl_2$, and 100 μM L-arginine, with pH 7.4) bubbled with 95% O_2-5% CO_2 at 37°C. Given that HEPES is a charged molecule that does not permeate the plasmalemma, CO_2 was included in the bubbled gas to stabilize intracellular pH. At specified intervals for each protocol, 1 ml of perfusate was collected, capped, and held on ice for 1 h to facilitate the conversion of NO to nitrite and nitrate (the stable metabolites of NO oxidation). Samples were lyophilized and stored at −20°C for subsequent nitrate determination (see *Determination of NO content in perfusates*). On completion of each perfusion protocol, each artery segment was removed from the chamber and its total soluble protein content was determined as previously described (32), with the use of Coomassie brilliant blue protein dye (catalog no. 500-0006; Bio-Rad).

To determine the effects of fluid shear stress on NO production, a single artery segment from each animal was sequentially perfused at 1, 2, and 4 ml/min. These flow rates yielded near-physiological levels of fluid shear stress (11) in both age groups but were low enough to avoid endothelial denudation and excessive dilution of sample NO levels. The height of the outflow cannula was varied to control inflow pressure independent of flow rate (Fig. 1). The inflow pressure was continuously measured with a pressure transducer and recorded online by computer. In preliminary experiments, NO release stabilized within a few minutes of any change in either flow or inflow pressure, and changes in inflow pressure between 20 and 60 mmHg had no significant effect on NO release. Thus arteries were perfused at each given flow rate at pressures between 20 and 60 mmHg for 10 min, and then aliquots of the perfusate were taken. This pattern was repeated for each flow rate.

To determine the effects of ADP and A-23187 on NO production, two adjacent segments of the same carotid artery were perfused with Na-HEPES buffer that contained 0.1 mM ADP or 0.1 mM A-23187 dissolved in 0.01% DMSO. As we have demonstrated previously via dose-response determinations, these concentrations yield maximal vasodilatation in ovine carotid arteries (33). The perfusate used in the vehicle controls for the A-23187 experiments contained only 0.01% DMSO in Na-HEPES buffer. To provide equivalent levels of shear stress for both preparations, both fetal and adult arteries were perfused at an average shear of 5.9 ± 0.6 dyn/cm^2. Arteries were exposed to flow for 20 min before the perfusion with ADP or A-23187. Aliquots of the perfusate were collected every 60 s for 6 min after the introduction of either ADP or A-23187.

Calculation of fluid shear stress. Fluid shear stress through perfused artery segments was calculated as described by Fung (14) as

$$\text{Shear stress (in dyn/cm}^2) = \frac{4 \times \mu \times \dot{Q}}{\pi r^2}$$

where μ is the perfusate viscosity (0.703 cP), $\dot{Q}$ is the flow velocity (in ml/s), and r is the radius of the individual perfused artery segment (in cm). The viscosity of the perfused buffer was determined by using a

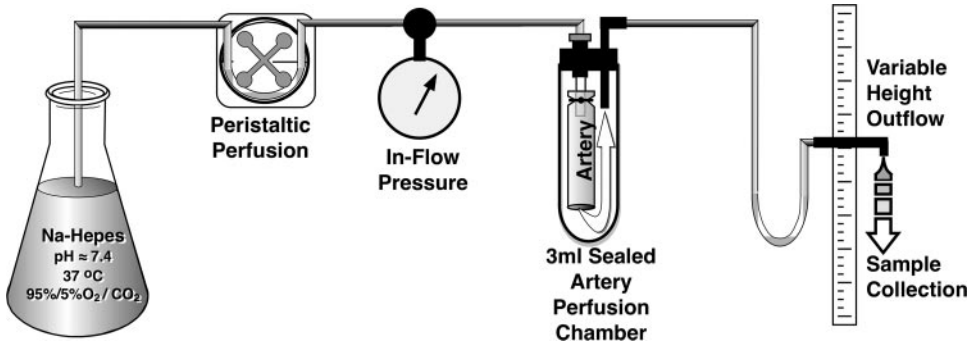

Fig. 1. Diagram of perfusion system. Fetal and adult ovine carotid arteries were mounted in a constant-volume, flow-through chamber with a variable outflow height that enabled independent control of flow and inflow pressure.

falling-ball viscometer (Gilmont Instruments) at 37°C. Shear stresses were calculated separately for each vessel segment used. Because of the uniformity of pressures within the perfusion chamber, artery diameters did not change significantly in response to changes in either inflow pressure or flow, and thus a single measurement of diameter was used for all calculations in each segment.

Determination of NO content in perfusates. Endothelial NO release was measured as the total nitrate plus nitrite (NOx) concentration in each aliquot of the perfusate. Total NOx content was determined by using a fluorometric nitrate reductase system coupled to the production of 2,3-diaminonapthalene (catalog no. 780051; Cayman Chemical). The assay was optimized for high-salt conditions, and samples were analyzed on a 96-well plate reader (HTS 7000 series; PerkinElmer) with an excitation filter of 360 nm and an emission filter of 430 nm. A separate standard curve was determined for each plate analyzed, and all standards underwent exactly the same process of lyophyllization and reconstitution as used for the unknowns.

Quantitative Western blot analysis of eNOS. Artery segments were homogenized in glass on glass mortars in extraction buffer that contained 150 mM NaCl, 50 mM Tris·HCl, 10 mM EDTA, 0.5% Tween 20, 0.1% β-mercaptoethanol, 0.1 mM PMSF, 5 μg/ml leupeptin, and 5 μg/ml aprotinin at pH 8.0. Homogenates were centrifuged at 12,500 *g*, and the soluble protein content of the supernatant was quantified (see *Artery perfusion*). A total of 20 μg of soluble protein from each sample was resolved on each lane of 8% SDS-PAGE gels. In addition to samples, each gel also contained five lanes of recombinant eNOS standard (catalog no. 360880; Cayman Chemical) that ranged from 8.32×10^{-5} to 3.32×10^{-3} μg of protein. Resolved proteins were transferred onto nitrocellulose membranes (Schleicher and Schuell; Protran Bioscience) and blocked with 5% milk at 4°C overnight. Membranes were then probed at 22°C for 90 min with a primary mouse anti-eNOS monoclonal antibody (catalog no. 610297; BD Transduction Laboratories) at a 1:3,000 titer. Membranes were washed and incubated for 1 h at 22°C with a secondary horseradish peroxidase-conjugated goat anti-mouse antibody (catalog no. 31430; Pierce) at a 1:150,000 titer. Blots were visualized by using SuperSignal Femto substrate (Pierce) and analyzed with a computer-based image-analysis system (ChemiImager; AlphaInnotech).

Immunohistochemistry for eNOS. Arteries were fixed overnight in 10% neutral-buffered formalin and embedded in paraffin. Sections were taken at 5-μm thickness and deparaffinized in a standard series of xylenes and graded alcohols. Antigen retrieval was performed in citrate buffer (2 mM citric acid, 9 mM sodium citrate, pH 6.0), and slides were heated in a microwave for 3 min at full power and then cooled at 22°C for 15 min. The slides were then incubated with ImmunoPure peroxidase suppressor (catalog no. 35000; Pierce) for 15 min, washed, and blocked in blocking buffer (1% BSA, 0.1 M PBS, 0.1% Triton X-100) at 22°C for 1 h. Sections were then incubated overnight at 4°C with the primary mouse monoclonal eNOS antibody (catalog no. 610297; BD Transduction Laboratories) at a 1:100 titer in 1% BSA. Negative-control sections were incubated in blocking buffer alone without primary antibody. All sections were washed and incubated with a secondary biotinylated horseradish peroxidase horse anti-mouse IgG (catalog no. 32028; Pierce) at a 1:220 titer in 1.3% normal horse serum for 2 h at 22°C. Sections were washed and subsequently incubated in avidin-biotin-peroxidase complex (catalog no. 32028, ABC kit; Pierce) for 30 min. The eNOS was visualized by using the substrate 3,3′-diaminobenzidene. Sections were subsequently counterstained with Harris-modified hematoxylin and eosin.

Measurement of eNOS mRNA. Artery segments were pulverized in liquid nitrogen and transferred to tubes that contained TRI Reagent (catalog no. T9424; Sigma) for 10 min of incubation at 22°C. Chloroform was then added, and the tubes were shaken and equilibrated for another 10 min. The samples were centrifuged at 12,000 *g* for 15 min at 4°C, after which the aqueous upper phase was decanted into tubes to which 100% isopropanol was also added (in a 1:1 ratio). After 15 min at 22°C, the samples were again centrifuged at 12,000 *g* for 15 min at 4°C to precipitate RNA. RNA pellets were washed with 70% ethanol, redissolved in diethyl pyrocarbonate-treated water, and treated with DNase (catalog no. 1906; Ambion). RNA concentrations were determined spectrophotometrically at 260 nm.

A two-step RT-PCR reaction was used to amplify eNOS mRNA. First-strand cDNA was generated by incubating 3 μg of total arterial RNA with nonspecific Oligo(dT) primers (catalog no. 18418020; Invitrogen) and RT (catalog no. 11731015, ThermoScript; GIBCO) at 55°C for 45 min and then for 5 min at 85°C. High temperature was necessary to prevent mRNA folding, and thus a high-temperature RT enzyme was used. After treatment with *Escherichia coli* RNase for 30 min at 37°C, RT products were transferred to the PCR reaction, which was run with *Taq* DNA polymerase and eNOS-specific primers (NCBI accession no. AF201926; Midland Certified Reagents). From 10^3 to 10^9 copies of 300-bp eNOS cDNA-inserted plasmid (NCBI accession no. U76738) were used in separate tubes as standards and positive controls. The relation between cycle number and product mass was examined between 28 and 40 cycles, each consisting of 30-s intervals at 94, 62, and 72°C. Optimum linearity was observed at 31 cycles.

RT-PCR products (samples and standards) were stained with SYBR Gold (catalog no. S11494; Molecular Probes) and separated on 2% agarose gels in TAE (Tris, acetic acid, and EDTA) running buffer at constant voltage (4 mV/cm of electrode distance) for 90–120 min. DNA markers, 72–1353 bp (catalog no. 1449460; Roche Molecular Biochemical), were also run on each gel. Bands for eNOS cDNA were detected at the 300-bp region, which is consistent with the location of our standard positive control. No bands were detected after eNOS PCR without prior reverse transcription (RT negative control), which indicates that DNA contamination was negligible. Integrated density values of both standard and unknown eNOS cDNA bands were measured by using an Alpha Innotech imaging system. Standard curves relating the plasmid copy numbers to integrated density values were constructed by using nonlinear regression, and from these curves, the eNOS mRNA copy numbers were determined by direct calculation based on sample optical densities.

Statistical analysis. The normality of sample distributions was verified by histogram plots with tests for skewness and kurtosis values using StatView 5.0. For independent two-sample comparisons, *F* ratios were determined, and none of these were significantly different than unity. Differences between experimental groups were analyzed by ANOVA with age, pressure, and shear stress as factors where appropriate. Homoscedasticity was verified by using a Cochran test. Slopes were determined by linear regression using StatView 5.0. To compare the coupling between shear stress and eNOS-specific activity in fetal and adult arteries, analysis of covariance was used to test for heterogeneity among the regression coefficients (slopes) and residual sums of squares for each computed line (36).

RESULTS

Throughout the text, all reported values indicate means and standard errors, and *n* refers to the number of animals. Unless stated otherwise, statistical significance implies $P < 0.05$. A total of 38 common carotid artery segments with a mean luminal diameter of 1.35 ± 0.04 cm were taken from 24 adult sheep, and a total of 31 segments with a mean luminal diameter of 0.86 ± 0.03 cm were taken from 21 fetal sheep for completion of these studies.

Effects of fluid shear stress on NO production. When adult artery segments were perfused at 1, 2, and 4 ml/min, the mean corresponding values of fluid shear stress averaged 1.3 ± 0.1, 2.7 ± 0.3, and 5.4 ± 0.5 dyn/cm^2, respectively. For fetal artery segments perfused at the same flow rates, the corresponding values of fluid shear stress averaged 6.3 ± 0.4, 12.7 ± 0.8, and 25.3 ± 1.7 dyn/cm^2. For both adult and fetal artery segments,

NO release normalized relative to luminal surface area increased with increasing fluid shear stress (Fig. 2). The effects of shear stress on NO release were significantly greater in adult than in fetal arteries for corresponding levels of either flow or fluid shear stress.

Effects of ADP and A-23187 on NO production. Perfusate NO concentrations, measured at 60-s intervals, were multiplied by their corresponding rates of perfusion (at 5.9 ± 0.6 dyn/cm^2 in both fetal and adult arteries) to calculate the rates of NO release during 6 min of administration of either ADP or A-23187 (Fig. 3*A*). In adult preparations, perfusion with 0.1 mM A-23187 stimulated an average NO release that was significantly greater than that produced in response to 0.1 mM ADP. This pattern was also observed in fetal preparations. NO release was also significantly greater in adult than in fetal arteries after treatment with A-23187 but not after treatment with ADP.

Abundance and localization of eNOS. For all blots used to quantify eNOS abundance, the optical densities obtained from the lanes containing recombinant eNOS standards were plotted against the mass of standard in each lane to produce a standard curve that was fitted to the logistic equation via nonlinear regression. The inverse function of the fitted equation was used to directly calculate eNOS abundances in each unknown lane. All sample optical densities were within the range defined by the standards as shown in Fig. 4*A*.

The abundances of eNOS relative to total soluble protein were significantly less in adult than in fetal artery segments (11 ± 2 vs. 29 ± 3 ng of eNOS/mg of total protein, respectively) as indicated in Fig. 4*A*. However, when eNOS abundances were normalized relative to luminal surface area, adult and fetal eNOS abundances were not significantly different (Fig. 4*B*). Immunohistochemistry revealed eNOS to be localized only within endothelial cells in both adult and fetal preparations (Fig. 5).

Abundance of eNOS mRNA. Standard curves relating the measured integrated optical density values to known numbers of plasmid copies of eNOS PCR product yielded sigmoidal relations with a half-maximal density obtained at $10^{6.1}$ copies. Total RNA yields averaged 149 ± 9 and 275 ± 25 μg/g wet wt in adult and fetal arteries, respectively. The relative abundances of eNOS mRNA averaged 7,170 ± 1,312 and 21,840 ± 6,570 copies/μg of total RNA. When expressed relative to total soluble protein, the eNOS mRNA values averaged (63 ± 12) × 10^6 and (209 ± 76) × 10^6 copies/mg of protein in adult and fetal arteries, respectively. However, when mRNA abun-

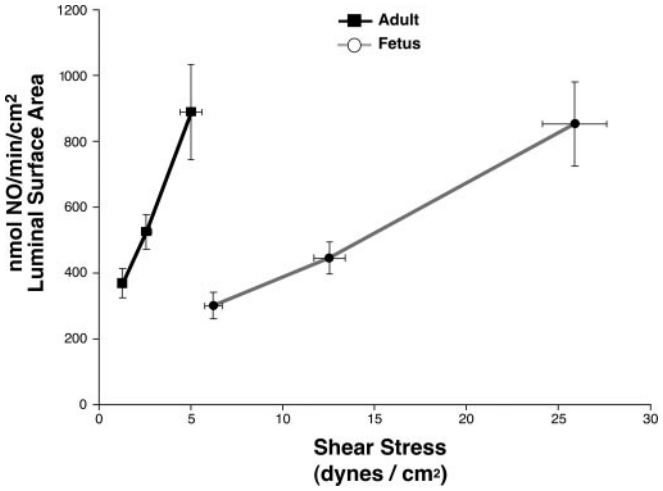

Fig. 2. Effects of age on fluid shear-induced nitric oxide (NO) release. Adult and fetal artery segments were perfused at three rates of fluid flow. NO release, normalized to luminal surface area, increased significantly with increasing rates of fluid shear stress in both adult and fetal arteries. For corresponding levels of fluid shear stress, NO release was significantly greater in adult than in fetal arteries. All values are means ± SE for 6 adult sheep and 8 fetal lambs at each indicated point.

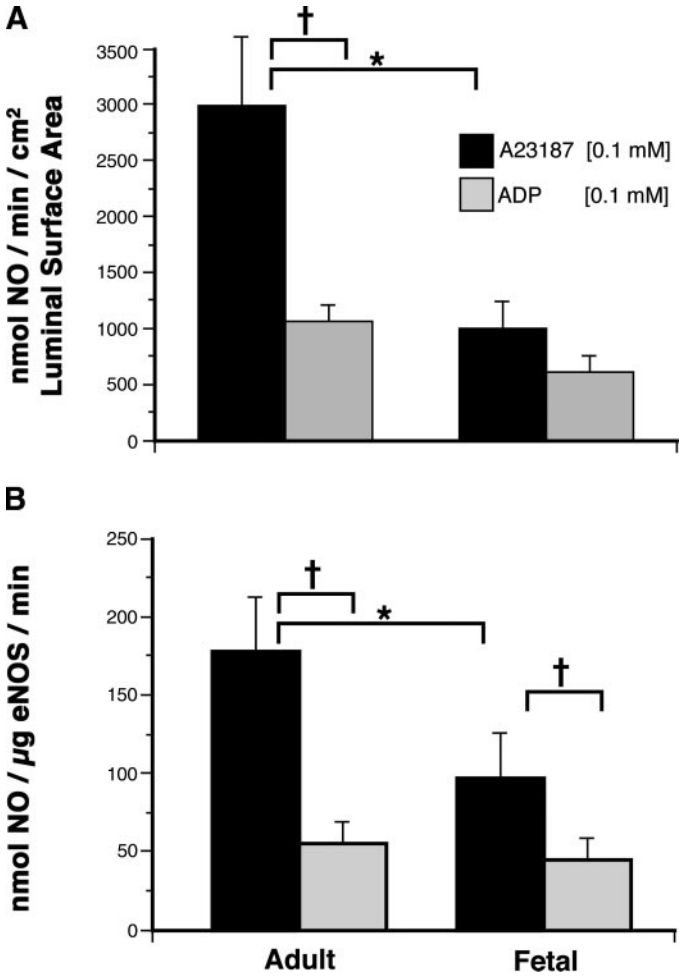

Fig. 3. Drug-induced NO release in perfused artery segments. *A*: average totals of NO release, normalized relative to luminal surface area, during 6 min of perfusion with Na-HEPES buffer that contained 0.1 mM A-23187 or 0.1 mM ADP. For each preparation from each animal, separate but adjacent artery segments were used for ADP and A-23187 perfusion. Adult and fetal arteries were perfused at similar rates of shear. Across both adult and fetal arteries, A-23187 stimulated an average NO release that was significantly greater than that produced in response to ADP (via ANOVA), but this difference was individually significant upon post hoc analysis only in the adult. Post hoc analysis further revealed that NO release was also significantly greater in adult than in fetal arteries after treatment with A-23187 but not after treatment with ADP. All values are means ± SE for 10 adult sheep and 8 fetal lambs. *B*: values of NO release shown in *A* were normalized to the measured abundances of endothelial NO synthase (eNOS) determined for each perfused artery segment. Average total NO release was measured during 6 min of perfusion with Na-HEPES buffer that contained 10^{-4} M A-23187 (black bars) or 10^{-4} M ADP (gray bars). Values are means ± SE for 8 adult sheep and 6 fetal lambs. *$P < 0.05$, significant difference between adult and fetal artery responses to treatment with A-23187; †$P < 0.05$, significant differences between treatments within age groups.

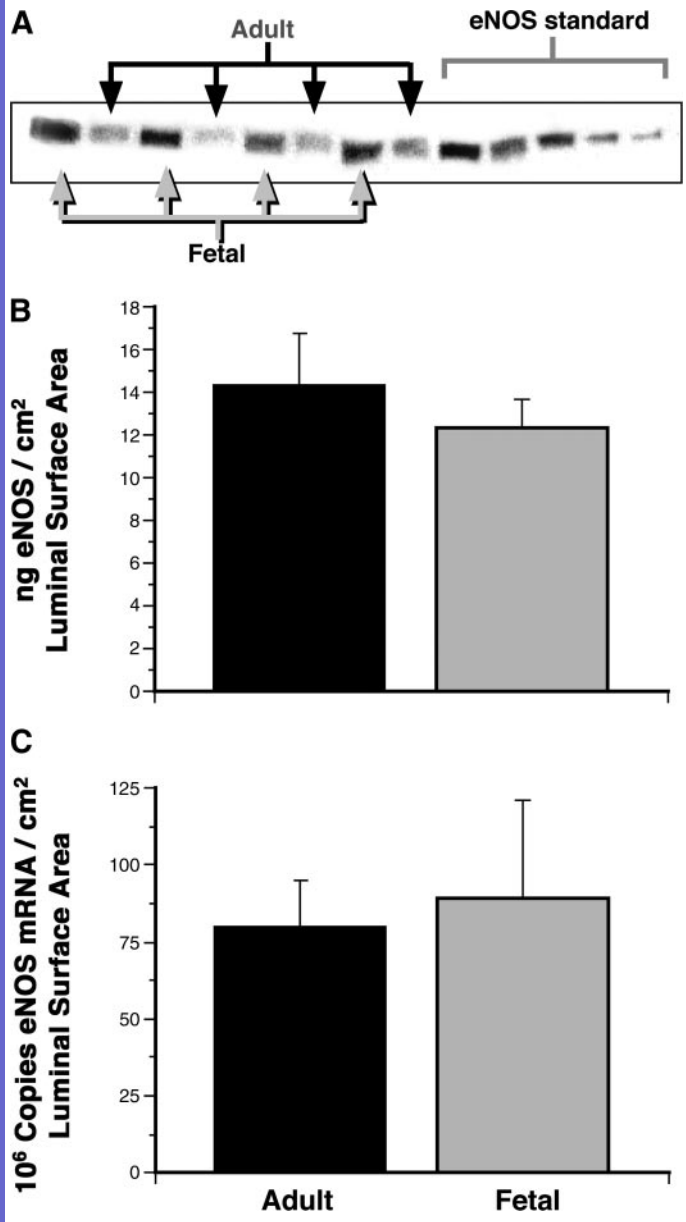

Fig. 4. Maturation depresses relative eNOS abundance. *A*: a Western blot result for eNOS abundance in adult and fetal carotid artery homogenates. Equivalent masses of total protein (20 μg) were loaded on each lane. Recombinant eNOS standards of (*right* to *left*) 8.32×10^{-5}, 1.66×10^{-4}, 4.16×10^{-4}, 1.66×10^{-3}, and 3.32×10^{-3} μg of protein per lane are also shown. *B*: results of densitometric quantification of eNOS abundance in adult and fetal preparations. Note that when eNOS abundances were normalized relative to total soluble protein, fetal values were significantly greater than adult values. When the results were normalized relative to luminal surface area, however, the age difference disappeared as shown. All values are means ± SE for 11 adult sheep and 9 fetal lambs. *C*: results of densitometric quantification of the abundance of eNOS mRNA in adult and fetal preparations. Values are means ± SE for 8 adult sheep and 7 fetal lambs.

dances were normalized relative to luminal surface area, adult and fetal values were not significantly different (see Fig. 4*C*). Correspondingly, calculations of the ratio of eNOS protein to mRNA yielded values of 175 ± 67 and 172 ± 82 ng of eNOS protein/10^6 copies of eNOS mRNA, and these values did not differ significantly.

Fluid shear and drug-induced release of NO normalized against eNOS abundance. To estimate the enzyme-specific activity of eNOS, the rate of NO production was normalized to the abundance of eNOS measured in each segment. In both adult and fetal arteries, eNOS-specific activity was significantly greater during treatment with A-23187 than during treatment with ADP (see Fig. 3*B*). During treatment with A-23187, eNOS-specific activity also was significantly greater in adult than in fetal arteries. In contrast, during treatment with ADP, eNOS-specific activity did not vary significantly with age.

The estimated specific activities of eNOS varied directly with fluid shear stress levels in both adult and fetal arteries, and the slopes of these relations were significantly greater in adult arteries (6.76 ± 0.07; $n = 6$) than in fetal arteries (2.85 ± 0.05; $n = 6$). Independent of absolute fluid shear stress levels, eNOS-specific activity was significantly greater in adult than in fetal arteries at each flow rate studied.

DISCUSSION

One of the most physiologically relevant stimulators of endothelial NO release is fluid shear stress (4, 8, 13). Shear stress can be applied to cultured endothelial cells, but endothelial phenotype is highly labile and can vary dramatically between cultured and in situ conditions (27). Such differences are particularly important when comparing arteries of different ages, because the phenotypes of both vascular smooth muscle and endothelial cells change rapidly during the postnatal period (26, 27). Because of these limitations, elucidation of the effects of postnatal maturation on endothelial reactivity and NO release is best realized by using intact perfused arteries. To this end, the closed perfusion system developed for the present studies enabled independent control of fluid shear stress and hydrostatic pressure. A key additional feature of this system was that it facilitated complete recovery of all NO released into the perfusate (see Fig. 1). Thus the perfusion system employed provided a unique and reasonable approximation of the conditions governing NO release in fetal and adult arteries and enabled unique observations not previously available in the literature.

The main hypothesis addressed by this study was that maturational increases in endothelium-dependent vasodilatation are mediated by corresponding increases in endothelial NO synthesis and release. Consistent with this hypothesis, the absolute rates of endothelial NO release were consistently greater in adult than in fetal arteries at corresponding rates of fluid shear stress (see Fig. 2). Conversely, these data also revealed that hydrostatic pressure did not significantly influence the extent of endothelial activation and NO release in either fetal or adult arteries. It remains possible, however, that the observed differences in NO release were attributable to age-related differences in the relative abundance of eNOS (23). The argument against this possibility was the finding that Western blot measurements revealed eNOS abundances were not significantly greater in adult than in fetal arteries (see Fig. 4), regardless of the method used to normalize abundance. Indeed, when eNOS abundance was normalized relative to either artery weight or milligrams of protein, abundance was greater in fetal than in adult arteries, a result we attributed to much greater adventitial mass in the adult arteries. However,

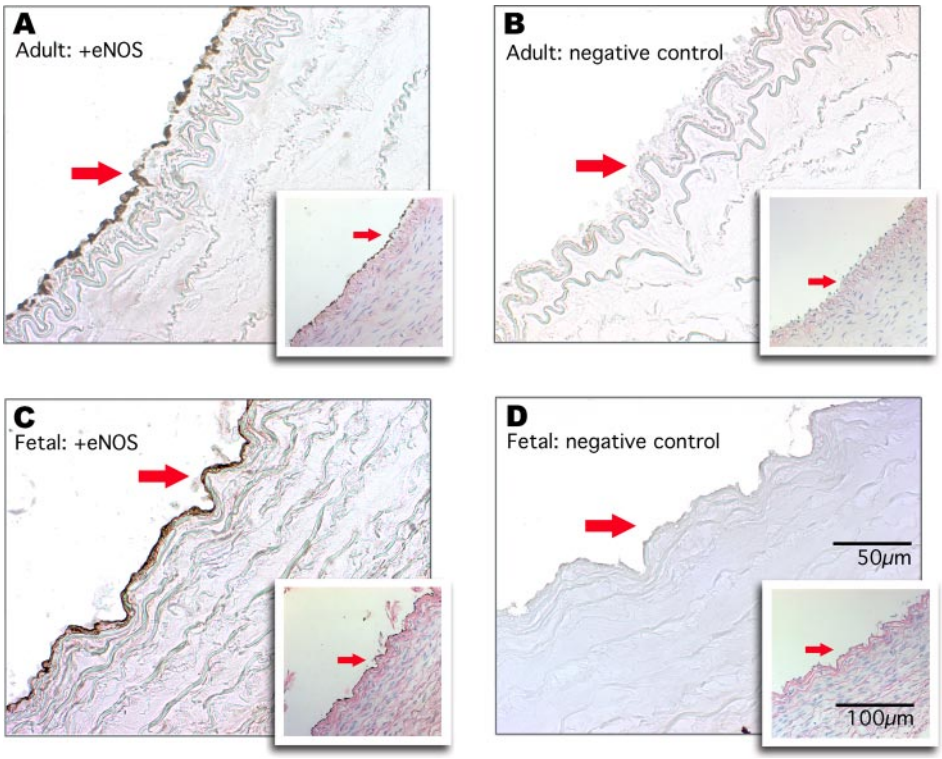

Fig. 5. Immunohistochemistry for eNOS localization in adult and fetal carotids. In these primary microphotographs, dark brown staining of the endothelial monolayer along the interior luminal surface of common carotid arteries indicates eNOS-positive cells. The lower power fields of view indicate the same tissues counterstained with hematoxylin and eosin (*insets*). Positional references between the primary micrographs and *insets* are shown (arrows). *A* and *C*: positive staining for eNOS in adult and fetal arteries, respectively. *B* and *D*: corresponding negative controls.

when eNOS abundance was normalized relative to luminal surface area, age-related differences became insignificant (see Fig. 4*B*), which suggests that perhaps average eNOS density may be a regulated variable. More importantly, this result suggests that normalization of NO release relative to luminal surface area (see Fig. 3*A*) minimized variability due to possible age-related differences in eNOS abundance. Similarly, eNOS mRNA abundances, normalized relative to luminal surface area (see Fig. 4*C*), were also similar in fetal and adult arteries as were the ratios of eNOS mRNA to eNOS protein, which indicates that the rates of eNOS transcription and the efficiency of message translation probably change little with postnatal age. Equally important, immunohistochemistry revealed that all eNOS protein was localized to the endothelial layer (see Fig. 5), such that age-related differences in NO production could not be attributed to an extra-endothelial distribution of fetal eNOS. Together, these findings strongly suggest that the greater ability of adult arteries to release NO was not due a greater relative abundance of eNOS protein in the endothelium of adult compared with fetal arteries.

Without doubt, comparisons of protein abundance among arteries of different ages are complicated by maturational differences in endothelial and smooth muscle cell size, cell number, hydration, artery diameter, and wall thickness (12, 25). Normalization relative to total cellular protein can be influenced by large differences in artery wall thickness and the ratio of artery wall mass per endothelial cell, such as those that exist between fetal and adult ovine carotid arteries (25, 33). Correspondingly, when the abundances of eNOS protein and mRNA were normalized relative to total soluble artery protein, fetal values were significantly greater than adult values. However, when these abundances were normalized relative to luminal surface area, which better represents the functional density of eNOS, there were no age-related differences in the abundances of either eNOS mRNA or protein. Together, these findings suggest that the functional density of the eNOS enzyme in the endothelial monolayer is probably regulated to remain relatively constant throughout postnatal maturation.

Aside from eNOS abundance, another key determinant of total endothelial NO release is the specific activity of the eNOS enzyme. Given this, our second corollary proposes that age-related changes in eNOS-specific activity contribute to corresponding postnatal differences in NO release. To test this possibility, we normalized the NO release measured in each segment studied relative to the mass of eNOS present in that segment. This approach yielded unique estimates of eNOS-specific activity in situ that were independent of maturational differences in artery composition. More importantly, the slopes of the relations between estimated eNOS-specific activity and fluid shear stress remained significantly greater in adult than in fetal arteries (Fig. 6). This result implies that the ability of fluid shear stress to activate eNOS is significantly greater in adult than in fetal arteries. These differences in eNOS activation in turn could be due to either greater mechanical sensitivity to fluid shear stress and/or greater reactivity of eNOS to activating stimuli in adult compared with fetal arteries.

Whereas the controversial nature of the mechanisms mediating mechanotransduction complicates any direct measurements of endothelial mechanical sensitivity (2, 10), it is much more straightforward to assess the reactivity of eNOS to activating stimuli. To that end, inclusion of the calcium ionophore A-23187 in the perfusate elicited a rapid, robust, and maximal stimulation of NO output in both fetal and adult arteries (see Fig. 3*A*). This result was completely consistent with the well-documented profile of A-23187 action as a receptor-independent mediator of maximal calcium entry into

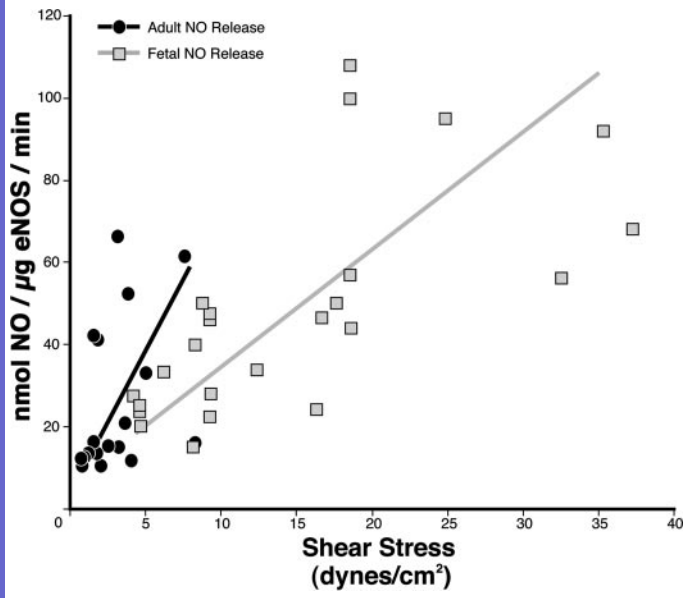

Fig. 6. Responses of eNOS-specific activity to fluid shear. Values of NO release shown in Fig. 2 were normalized to the measured abundances of eNOS determined for each perfused artery segment. Absolute value of fluid shear stress varied depending upon the internal lumen diameter of each individual perfused artery segment and the rate of flow used for that segment. Given that perfusion pressure had no effect on shear-induced NO release, no distinction was made for segments perfused at different pressures. Values for eNOS-specific activity were plotted individually at each given level of fluid shear stress obtained in arteries from 6 adult sheep and 8 fetal lambs.

endothelial cells (29). More importantly, the NO output elicited by A-23187 was significantly greater in adult than in fetal arteries and was also significantly greater than that observed in response to fluid shear stress in either age group. This pattern of effects persisted even after NO output had been normalized to eNOS abundance to estimate eNOS-specific activity (see Fig. 3*B*). The fact that the patterns of age-related differences in both total NO output and eNOS-specific activity were highly similar further suggests that significant age-related differences in the reactivity of eNOS to activating stimuli strongly influence the corresponding age-related differences in total NO release.

Previous studies have also shown that eNOS-specific activity can be physiologically modulated. For example, Iwakiri et al. (17) have shown in hypertensive rats that physiological reductions in eNOS-specific activity are due to phosphorylation of eNOS by Akt kinase. Clearly, eNOS is a well-established target for Akt kinase (6), but the participation of this pathway in immature endothelium remains unexplored. Given that the phosphatidylinositol 3-kinase/Akt system is activated by growth factors and estrogen (7, 16), both of which in turn are elevated in immature vascular tissues, it seems reasonable to speculate that age-related differences in phosphatidylinositol 3-kinase/Akt activity may be involved. Alternatively, protein kinase C can also catalyze an inhibitory phosphorylation of eNOS (20), and the expression and activity of protein kinase C also change significantly during development and postnatal maturation (35). It further remains possible that age-related changes in eNOS-specific activity may arise from differential expression of eNOS splice variants. Although alternative splice variants have been demonstrated for other NOS isoforms (1), age-related changes in splicing isoforms have yet to be demonstrated for eNOS.

In contrast with A-23187, ADP-induced stimulation of eNOS exhibited far more subtle age-related differences (see Fig. 3). Indeed, both total NO release and eNOS-specific activity after stimulation with a physiologically maximal concentration of ADP were not significantly different in fetal and adult arteries. Assuming that eNOS-specific activity in the presence of A-23187 provided an index of maximal activation, the activity observed in response to ADP expressed relative to that for A-23187 was taken as an estimate of fractional activation of eNOS. Correspondingly, the ADP results suggested that fractional activation of eNOS in response to ADP was upregulated in fetal compared with adult arteries. Such differences, in turn, could potentially involve age-related differences in the density, agonist affinity, or coupling efficiency of the endothelial ADP receptors to eNOS (24). From a functional perspective, upregulation of the coupling between ADP and eNOS activation may compensate for the attenuated eNOS activity characteristic of immature arteries and could thus preserve the ability of physiological vasodilators such as ADP to stimulate endothelium-dependent vasodilatation in the fetus.

Overall, the combined results support our main hypothesis that age-dependent increases in endothelial vasodilator capacity are due to corresponding increases in NO synthesis and release. Because these results were obtained from whole arteries perfused under physiologically relevant conditions of shear stress, they most probably reflect underlying age-related differences in endothelial phenotype and function. The results, however, do not support our first corollary, that age-related differences in NO release are attributable to corresponding differences in eNOS abundance. Indeed, the results indicate that the functional distributions of eNOS protein and mRNA, when normalized relative to luminal surface area, were closely similar in fetal and adult arteries. Concerning our second corollary, which attributes age-related differences in NO release to corresponding differences in eNOS-specific activity, the results support this possibility. When in situ eNOS-specific activity was estimated by the ratio of maximal A-23187-induced NO release relative to eNOS abundance, eNOS-specific activity was consistently greater in adult than in fetal arteries, which suggests important possible age-related differences in the posttranslational regulation of eNOS. Regarding our third corollary, which attributes age-related differences in the ability of physiological and pharmacological stimuli to activate eNOS, the results were mixed. Maximal activation of eNOS-specific activity with A-23187 yielded greater rates of NO release in adult compared with fetal arteries. Similarly, the relations between fluid shear stress and eNOS-specific activity exhibited greater slopes in adult than in fetal arteries. Together, these findings suggest that eNOS may be more sensitive to activating stimuli in adult compared with fetal arteries. For ADP-induced NO release, however, fractional activation by ADP appeared greater in fetal than in adult arteries, which suggests possible upregulation of endothelial reactivity through changes in ADP receptor sensitivity, density, or coupling. Clearly, coupling of physiological stimuli to endothelial NO release involves multiple mechanisms that appear to be independently regulated. Most importantly, the regulation of these mechanisms appears to be age dependent, which suggests that further studies of this regulation may help provide insight

into the underlying reasons for age-related differences in cerebrovascular regulation and vulnerability to insult in the neonatal period.

ACKNOWLEDGMENTS

The authors thank James Williams for logistical work on this project. The authors also thank Dr. Lubo Zhang for insightful suggestions regarding interpretation of these data.

GRANTS

This work was supported by National Institutes of Health Grants HD-31226 and HL-64867.

REFERENCES

1. **Alderton WK, Cooper CE, and Knowles RG.** Nitric oxide synthases: structure, function and inhibition. *Biochem J* 357: 593–615, 2001.
2. **Ali MH and Schumacker PT.** Endothelial responses to mechanical stress: where is the mechanosensor? *Crit Care Med* 30: S198–S206, 2002.
3. **Anderson PA.** Maturation and cardiac contractility. *Cardiol Clin* 7: 209–225, 1989.
4. **Belardinelli R and Perna GP.** Vasomotor reactivity evaluation in cardiac rehabilitation. *Monaldi Arch Chest Dis* 58: 79–86, 2002.
5. **Berger R, Garnier Y, and Jensen A.** Perinatal brain damage: underlying mechanisms and neuroprotective strategies. *J Soc Gynecol Investig* 9: 319–328, 2002.
6. **Boo YC and Jo H.** Flow-dependent regulation of endothelial nitric oxide synthase: role of protein kinases. *Am J Physiol Cell Physiol* 285: C499–C508, 2003.
7. **Brouet A, Sonveaux P, Dessy C, Balligand JL, and Feron O.** Hsp90 ensures the transition from the early Ca^{2+}-dependent to the late phosphorylation-dependent activation of the endothelial nitric-oxide synthase in vascular endothelial growth factor-exposed endothelial cells. *J Biol Chem* 276: 32663–32669, 2001.
8. **Busse R and Fleming I.** Pulsatile stretch and shear stress: physical stimuli determining the production of endothelium-derived relaxing factors. *J Vasc Res* 35: 73–84, 1998.
9. **Charpie JR, Schreur KD, Papadopoulos SM, and Webb RC.** Endothelium dependency of contractile activity differs in infant and adult vertebral arteries. *J Clin Invest* 93: 1339–1343, 1994.
10. **Chiu YJ, Kusano K, Thomas TN, and Fujiwara K.** Endothelial cell-cell adhesion and mechanosignal transduction. *Endothelium* 11: 59–73, 2004.
11. **Davies PF.** Flow-mediated endothelial mechanotransduction. *Physiol Rev* 75: 519–560, 1995.
12. **Elliott CF and Pearce WJ.** Effects of maturation on cell water, protein, and DNA content in ovine cerebral arteries. *J Appl Physiol* 79: 831–837, 1995.
13. **Frangos JA, Huang TY, and Clark CB.** Steady shear and step changes in shear stimulate endothelium via independent mechanisms—superposition of transient and sustained nitric oxide production. *Biochem Biophys Res Commun* 224: 660–665, 1996.
14. **Fung Y.** *Biomechanics: Circulation* (2nd ed.). New York: Springer, 1996, p. 114–118.
15. **Garlanda C and Dejana E.** Heterogeneity of endothelial cells. Specific markers. *Arterioscler Thromb Vasc Biol* 17: 1193–1202, 1997.
16. **Haynes MP, Sinha D, Russell KS, Collinge M, Fulton D, Morales-Ruiz M, Sessa WC, and Bender JR.** Membrane estrogen receptor engagement activates endothelial nitric oxide synthase via the PI3-kinase-Akt pathway in human endothelial cells. *Circ Res* 87: 677–682, 2000.
17. **Iwakiri Y, Tsai MH, McCabe TJ, Gratton JP, Fulton D, Groszmann RJ, and Sessa WC.** Phosphorylation of eNOS initiates excessive NO production in early phases of portal hypertension. *Am J Physiol Heart Circ Physiol* 282: H2084–H2090, 2002.
18. **Kolber KA, Gao Y, and Raj JU.** Maturational changes in endothelium-derived nitric oxide-mediated relaxation of ovine pulmonary arteries. *Biol Neonate* 77: 123–130, 2000.
19. **Lucey JF, Rowan CA, Shiono P, Wilkinson AR, Kilpatrick S, Payne NR, Horbar J, Carpenter J, Rogowski J, and Soll RF.** Fetal infants: the fate of 4,172 infants with birth weights of 401 to 500 grams—the Vermont Oxford Network experience (1996–2000). *Pediatrics* 113: 1559–1566, 2004.
20. **Matsubara M, Hayashi N, Jing T, and Titani K.** Regulation of endothelial nitric oxide synthase by protein kinase C. *J Biochem (Tokyo)* 133: 773–781, 2003.
21. **McGowan FXJ, Davis PJ, del Nido PJ, Sobek M, Allen JW, and Downing SE.** Endothelium-dependent regulation of coronary tone in the neonatal pig. *Anesth Analg* 79: 1094–1101, 1994.
22. **Nauli SM, White CR, Hull AD, and Pearce WJ.** Maturation alters cyclic nucleotide and relaxation responses to nitric oxide donors in ovine cerebral arteries. *Biol Neonate* 83: 123–135, 2003.
23. **Parfenova H, Massie V, and Leffler CW.** Developmental changes in endothelium-derived vasorelaxant factors in cerebral circulation. *Am J Physiol Heart Circ Physiol* 278: H780–H788, 2000.
24. **Pearce WJ.** Pharmacomechanical coupling in the cerebral circulation. In: *Cerebral Blood Flow and Metabolism*, edited by Edvinsson L and Krause D. Philadelphia, PA: Lippincott, Williams, and Wilkins, 2002, p. 88–106.
25. **Pearce WJ, Hull AD, Long DM, and Longo LD.** Developmental changes in ovine cerebral artery composition and reactivity. *Am J Physiol Regul Integr Comp Physiol* 261: R458–R465, 1991.
26. **Ratajska A, Zarska M, Quensel C, and Kramer J.** Differentiation of the smooth muscle cell phenotypes during embryonic development of coronary vessels in the rat. *Histochem Cell Biol* 116: 79–87, 2001.
27. **Risau W.** Differentiation of endothelium. *FASEB J* 9: 926–933, 1995.
28. **Seri I and Evans J.** Controversies in the diagnosis and management of hypotension in the newborn infant. *Curr Opin Pediatr* 13: 116–123, 2001.
29. **Taniguchi H, Tanaka Y, Hirano H, Tanaka H, and Shigenobu K.** Evidence for a contribution of store-operated Ca^{2+} channels to NO-mediated endothelium-dependent relaxation of guinea-pig aorta in response to a Ca^{2+} ionophore, A-23187. *Naunyn Schmiedebergs Arch Pharmacol* 360: 69–79, 1999.
30. **Thompson LP and Weiner CP.** Acetylcholine relaxation of renal artery and nitric oxide synthase activity of renal cortex increase with fetal and postnatal age. *Pediatr Res* 40: 192–197, 1996.
31. **Vanhoutte PM and Miller VM.** Heterogeneity of endothelium-dependent responses in mammalian blood vessels. *J Cardiovasc Pharmacol* 7, *Suppl* 3: S12–S23, 1985.
32. **White CR and Pearce WJ.** Effects of maturation on cyclic GMP metabolism in ovine carotid arteries. *Pediatr Res* 39: 25–31, 1996.
33. **Williams JM, Hull AD, and Pearce WJ.** Maturational modulation of endothelium-dependent vasodilatation in ovine cerebral arteries. *Am J Physiol Regul Integr Comp Physiol* 288: R149–R157, 2005.
34. **Willis AP and Leffler CW.** Endothelial NO and prostanoid involvement in newborn and juvenile pig pial arteriolar vasomotor responses. *Am J Physiol Heart Circ Physiol* 281: H2366–H2377, 2001.
35. **Yoshida T, Ichikawa Y, Ito K, and Homma M.** Monoclonal antibodies to the thyrotropin receptor bind to a 56-kDa subunit of the thyrotropin receptor and show heterogeneous bioactivities. *J Biol Chem* 263: 16341–16347, 1988.
36. **Zar J.** *Biostatistical Analysis* (4th ed.). New Jersey: Prentice Hall, 1999, p. 360–376.
37. **Zhang Y and Leffler CW.** Compensatory role of NO in cerebral circulation of piglets chronically treated with indomethacin. *Am J Physiol Regul Integr Comp Physiol* 282: R400–R410, 2002.